

# Adsorption of Gold on Iridium

**Khalil Ismaiel Hashim**

Physics Department, Faculty of Science, Benghazi University, Benghazi, Libya

Email: khalilismaiel@gmail.com

**How to cite this paper:** Hashim, K.I. (2018) Adsorption of Gold on Iridium. *Journal of Applied Mathematics and Physics*, 6, 1324-1331.

<https://doi.org/10.4236/jamp.2018.66111>

**Received:** June 6, 2018

**Accepted:** June 25, 2018

**Published:** June 28, 2018

Copyright © 2018 by author and Scientific Research Publishing Inc.

This work is licensed under the Creative Commons Attribution International License (CC BY 4.0).

<http://creativecommons.org/licenses/by/4.0/>



Open Access

---

## Abstract

The work described in this paper is a study of gold adsorption on the whole tip surface of iridium field emitter. The study has been carried out using field emission microscope. Changes in electron work function of the iridium substrate which are produced by vapor of deposition of submonolayers of gold in ultra high vacuum have been measured by noting the changes in the slope of Fowler-Nordheim plots. The same procedure for studying the adsorption of copper on iridium [1] was followed to study the adsorption of gold on iridium. Adsorption of gold was examined on the iridium surface containing the (100) ring which could not be removed thermally.

## Keywords

Field Emission Microscope, Electron Work Function, Fowler-Nordheim Plots, Co-adsorption, Pulsed Temperature-Field (T-F) Emission Microscopy, Low Energy Electron Diffraction (LEED), Auger Electron Spectroscopy (AES), Field Ion Microscopy (FIM)

---

## 1. Introduction

The field emission microscope (fem) was invented by Muller in 1937 [2]. He was the first person to experimentally observe atoms. This device is an analytical technique used in material science to investigate molecular structures and their electronic properties [3]. One of the most important applications of field emission microscope is the study of adsorption on metallic cathode surface. Such studies provide a powerful approach to problems in catalysis and surface chemistry.

A low work function surface, which is of technical interest, can be obtained by the co-adsorption of gas which decreases the emitter work function below that due to adsorption of the metallic adsorbate alone. Thus the understanding of the adsorption is a prerequisite to the development of methods for controlling the

electrical behaviour of the cathode for use in practical electronic devices [4].

Many other techniques are now available to study the adsorption phenomena in addition to field emission microscopy, for example, Pulsed Temperature-Field (T-F) emission microscopy, Low Energy Electron Diffraction (LEED), Auger Electron Spectroscopy (AES), and the Field Ion Microscopy (FIM). A comprehensive review of these techniques has been given by Gomer [5] and Coles [6].

Gold, which is adsorbed on iridium in the present study, crystallizes (as copper and silver) with face-centered cubic (fcc) structure. Simple field emission microscopy was used previously to study the adsorption of group 1b elements (copper, silver, and gold) on tungsten which has a body-centred cubic (bcc) structure and rhenium which has hexagonal close-packed (hcp) structure [7] [8], so in this study we have used iridium as a substrate because it has the fcc structure which is isomorphous with that of the bulk adsorbate.

## 2. Experimental

Before talking about the experimental procedure we give a brief review of how the field emission microscope works. **Figure 1** is a schematic diagram of a simple field emission microscope, as it can be seen, it consists of an evacuated glass bulb, the end face of which is covered with a conducting tin oxide layer which acts as an anode, and a layer of phosphor which serves as a screen. The specimen in the form of a sharp point (tip) acts as the cathode. To obtain a high field ( $3 - 7 \times 10^6$  volts/ cm) required for electron emission from the point, it is etched electrolytically to about  $1000 \text{ \AA}$  radius. The field ( $F$ ) at the surface of a free space sphere of radius  $r$  and potential  $V$  is given by [9]

$$F = V/r \quad (1)$$

At the surface of the tip the field ( $F$ ) is reduced by the presence of the shank and it can be approximated to

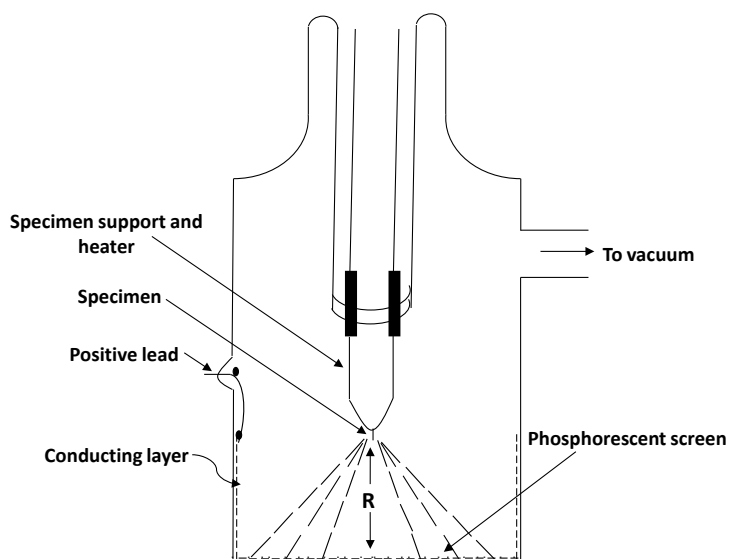


**Figure 1.** A schematic diagram of a simple field emission microscope.

$$F = V/kr \quad (2)$$

where  $r$  is the mean radius of the tip and  $k$  is the field reduction factor which has a value of about 5 near the apex and increases with polar angle [10].

When the field emitted electrons become free, they have essentially no kinetic energy [11] [12] in the emission direction and they follow the lines of force of the applied electric field travelling through the vacuum to impinge upon the phosphor screen producing an enlarged image of the tip surface. A field emission pattern usually consists of bright and dark areas depending on the flux density of the emitted electrons reaching the screen from different planes of the tip surface. Planes of low work function appear brighter than other higher work function regions.

Ideally the magnification would be given by  $R/r$  [12], however, due to the presence of the emitter shank, the actual magnification is given by [4] [10]

$$M = R/\alpha r \quad (3)$$

where ( $\alpha$ ) usually lies between the values of (1.5) and (2) [4] [10] [13] [14] [15] and arises from the fact that the emitter shank decreases the field and compresses the lines of force toward the axis so that the image is almost uniformly compressed with axial symmetry over the displaced portion of the emitter. In general, an average magnification of the order of  $10^5$  to  $10^6$  is obtained [12].

The large magnification of the microscope could be of a little value if the resolution was not proportionally good. The resolution of a field emission microscope is defined as the minimum distance between two objects on the tip surface that will produce separable images on the screen [10] [14] [16] [17]. A resolution in the order of 20 Å is usually obtained in a field emission microscope [10] [12] [18].

The study of gold adsorption on the total tip surface of iridium was conducted as follows: The thermally cleaned tip was held at 78 K by cooling it with liquid nitrogen, in the absence of the applied electric field, small doses of gold were successively deposited on the iridium emitter and evenly spread over the surface of the emitter by heating the supporting loop at a predetermined temperature for 60 seconds, the time which experiments showed was sufficient for a quasi-equilibrium state to be reached. By measuring the voltage ( $V$ ) required to draw a certain field emission current before deposition and after equilibrium of the adsorbate, the voltage ( $V$ ) versus coverage ( $\theta$ ) curve was plotted at every spreading temperature (Ts). FN readings were taken when the tip surface was clean ( $\theta = 0$ ) and at every third or fourth equilibrated dose afterwards. The resulting electron work function ( $\Phi$ ) was measured at those points. This procedure was repeated until there was no further change in ( $\Phi$ ) with gold adsorption. At this stage the tip was flash cleaned to remove the adsorbate gold and the whole process was repeated for a different spreading temperature.

### 3. Results and Discussion

#### Variation of Electron Work Function ( $\Phi$ ) with Gold Coverage ( $\theta$ )

( $\Phi$ - $\theta$ ) curves have been obtained at two spreading temperatures 500 K and 556 K

respectively. **Figure 1** depicts the ( $\Phi$ - $\theta$ ) characteristics at spreading temperature of 500 K ( $T_s = 500$  K) and it shows that ( $\Phi$ ) increases from 5.27 eV for clean iridium to a maximum value ( $\Phi$  max) of 5.39 eV at  $\theta = 0.7$  followed by a decrease to a minimum value ( $\Phi$  min) of 5.24 eV at  $\theta = 1.4$ . Addition of more gold increases ( $\Phi$ ) slowly to attain a value of 5.29 eV at  $\theta = 2.1$  where it remains coverage-independent ( $\Phi$  sat).

The shape of ( $\Phi$ - $\theta$ ) curve at spreading temperature of 556 K ( $T_s = 556$  K) which is illustrated in **Figure 3** resembles that at  $T_s = 500$  K (**Figure 2**), but ( $\Phi$  min) at this temperature is 5.10 eV and occurs at  $\theta = 2.1$  followed by an increase to 5.16 at  $\theta = 2.8$  where it decreases once more to attain ( $\Phi$  sat) of 5.10 eV at  $\theta = 3.5$ .

The thermally cleaned iridium tip used in this study contained the bright ring around the (100) plane from the early stages of the work, thus all the work reported has been carried out in the presence of the ring.

The first part of ( $\Phi$ - $\theta$ ) curves of our results at  $T_s = 500$  K and  $T_s = 556$  K which are depicted in **Figure 2** and **Figure 3** respectively has shown an increase in ( $\Phi$ ) with ( $\theta$ ) to a maximum value ( $\Phi$  max) at a coverage  $\theta = 0.7$ . The gold atom has an electronegativity of (2.4) [19] and when it is adsorbed on iridium which has an electronegativity of (2.2) [19], it forms an iridium-gold dipole in which gold is negatively charged with respect to iridium and this leads to a higher work function than that of the clean iridium.

It seems probable that differences in the distribution of the gold adatoms on the iridium substrate at 500 K and 556 K are responsible for the small differences in the values of ( $\Phi$  max).

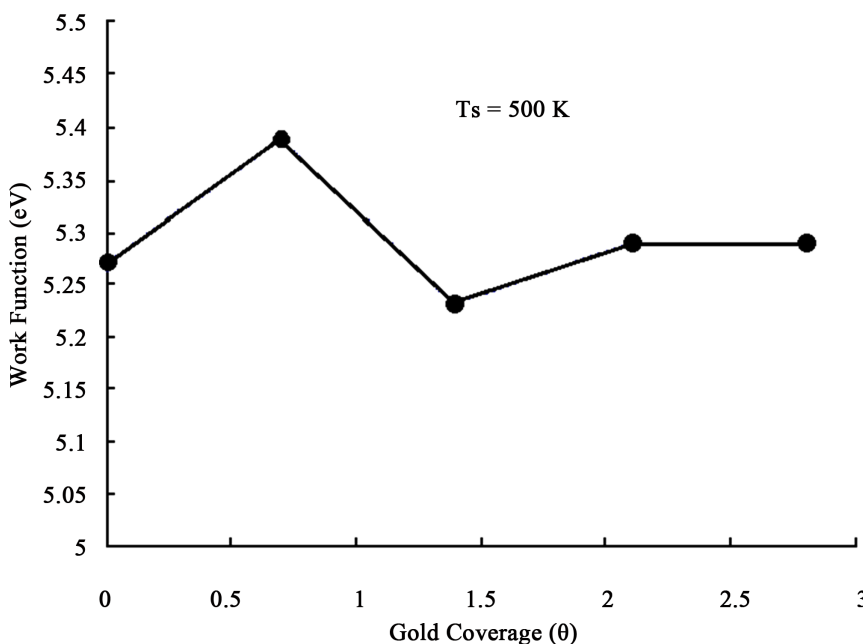


**Figure 2.** Change in work function of iridium tip surface with gold coverage ( $\theta$ ) at spreading temperature ( $T_s$ ) 500 K.

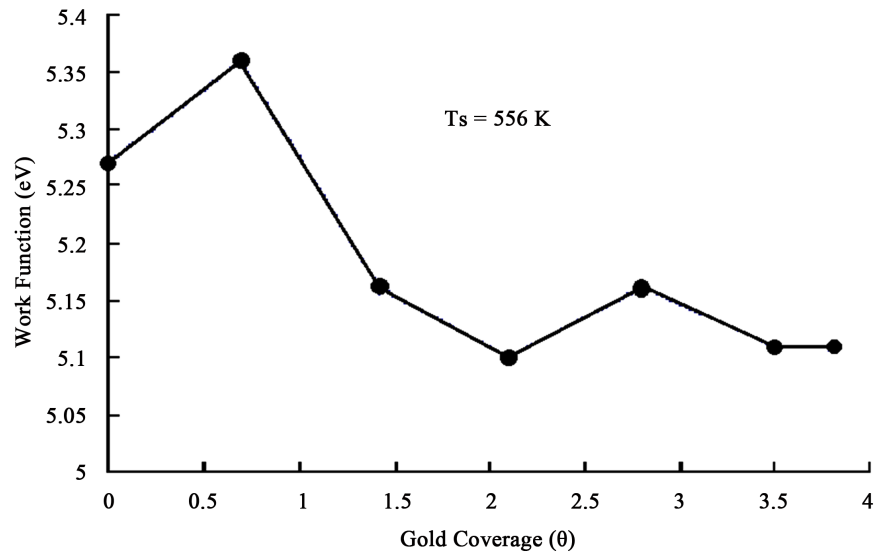


**Figure 3.** Change in work function of iridium tip surface with gold coverage ( $\theta$ ) at spreading temperature ( $T_s$ ) 556 K.

With increasing the adatom coverage, our results at  $T_s = 500$  K and  $T_s = 556$  K have shown a minimum in the work function value at about  $\theta = 1.4$  and  $\theta = 2.1$  respectively. The reduction in ( $\Phi$ ) at this stage may be attributed to a steady decrease in the influence of the substrate on the properties of gold layer resulting in a reduction in the influence of the electronegativity dipoles.

With further addition of gold at the both spreading temperatures our results show an increase in ( $\Phi$ ). At  $T_s = 500$  K with further coverage, ( $\Phi$ ) remains unchanged at the value of 5.3 eV, but at  $T_s = 556$  K ( $\Phi$ ) displays another decrease before it becomes a coverage-independent at a value of about 5.1 eV.

Our results of ( $\Phi$  sat) of gold adsorption on iridium total emitter surface are shown to be in agreement with the results of the other workers [20] [21] [22] [23]. A value of 5.1 eV was observed by [24]-[29], while Farrer *et al.* [30] and Trouwborst *et al.* [31] observed that the value of the work function of gold was less than 5.1 eV which is less than our value. Abid *et al.* [32] observed a value of 5.2 eV which is in the range of our values. Park *et al.* [33] observed values in the range of 5.1 - 5.3 eV which are in a good agreement with our value. Frederiksen *et al.* [34] found the values of the gold work function to be in the range of 5.31 - 5.41 eV which are higher than our measured value. Salisbury *et al.* [35] adopted a value of 5.5 eV for the work function of gold which is much higher than the value we obtained in our study.

#### 4. Conclusions

1) Adsorption of gold on the total surface of the iridium tip increases the average work function ( $\Phi$ ) at low coverage. This increase in ( $\Phi$ ) is expected if the electronegativity differences between the two atoms are considered. Gold has an electronegativity of (2.4) [19], while iridium has an electronegativity of (2.2)

[19]. Thus gold-iridium dipoles should be formed with gold which is negatively charged with respect to iridium, leading to the observed increase in ( $\Phi$ ).

The difference between ( $\Phi$  max) and ( $\Phi$  clean) is very small at 500 K and 556 K. The small variation between ( $\Phi$  max) values at 500 K and at 556 K may be attributed to the differences in the distribution of gold adatoms on the iridium surface.

( $\Phi$  sat) at  $T_s = 556$  K is found to be 5.10 eV in agreement with those values found by the others [24]-[29]. This value lies close to that obtained by Huber [22] (5.22 eV) using Contact Potential Difference, Jones *et al.*, [20], and Jones *et al.* [21] in their studies of gold adsorption on tungsten obtained values of 5.23 eV and 5.20 eV respectively, but our results do not agree with the values obtained by Frederiksen *et al.* [34] and Salisbury *et al.* [35].

2) We suggest more researches to be done on such systems, like adsorption of gold on other metal substrates and adsorption of other metals on gold substrate. Such studies might give better results and interpretations and consequently a better understanding of those systems.

## References

- [1] Hashim, K.I. (2017) Adsorption of Copper on Iridium. *Science and Its Applications*, **5**, 103-105.
- [2] Muller, EW. (1937) Elektronenmikroskopische Beobachtungen von Feldkathoden. *Zeitschrift für Physik*, **106**, 541-550. <https://doi.org/10.1007/BF01339895>
- [3] Semerci, E. (2011) Field Emission Microscope (FEM). *Journal of Materials Science and Technology*.
- [4] Dyke, W.P. and Dolan, W.W. (1956) Field Emission. *Advances in Electronics and Electron Physics*, **8**, 89-185. [https://doi.org/10.1016/S0065-2539\(08\)61226-3](https://doi.org/10.1016/S0065-2539(08)61226-3)
- [5] Gomer, R. (1967) Fundamental of Gas-Surface Interactions. Academic Press, New York, London.
- [6] Coles, S.J.T. (1976) Adsorption of Gold on Low Index Planes of Rhenium. Ph.D. Thesis, University College of Wales, Bangor.
- [7] Cetronio, A. and Jones, J.P. (1973) Reconstruction at a Metallic Interface Studied by Field Ion and Field Emission Microscopy. *Surface Science*, **40**, 227-248. [https://doi.org/10.1016/0039-6028\(73\)90065-4](https://doi.org/10.1016/0039-6028(73)90065-4)
- [8] Cetronio, A. and Jones, J.P. (1974) A Study by High Field Microscopy of the Effect of Substrate Surface Structure on the Work Function of Layers of Group 1B Metals Adsorbed on Tungsten. *Surface Science*, **44** 109-128. [https://doi.org/10.1016/0039-6028\(74\)90096-X](https://doi.org/10.1016/0039-6028(74)90096-X)
- [9] Gomer, R. (1961) Field Emission and Field Ionization. Harvard University Press, Cambridge.
- [10] Melmed, A.J. (1967) Surface Self-Diffusion of Nickel and Platinum. *Journal of Applied Physics*, **38**, 1885.
- [11] Russel, A.M. (1962) Electron Trajectories in a Field Emission Microscope. *Journal of Applied Physics*, **33**, 970. <https://doi.org/10.1063/1.1777199>
- [12] Gomer, R. (1978) Application of Field Emission to Chemisorption. *Surface Science*, **70**, 19-31. [https://doi.org/10.1016/0039-6028\(78\)90398-9](https://doi.org/10.1016/0039-6028(78)90398-9)

- [13] Van Oostrom, A. (1966) Validity of Fowler-Nordheim Model for Field Electron Emission. *Philips Research Reports*, 1-102.
- [14] Muller, E.W. (1960) Field Ionization and Field Ion Microscopy. *Advances in Electronics and Electron Physics*, **13**, 83-179. [https://doi.org/10.1016/S0065-2539\(08\)60210-3](https://doi.org/10.1016/S0065-2539(08)60210-3)
- [15] Rose, D.J. (1956) On the Magnification and Resolution of Field Electron Emission Microscope. *Journal of Applied Physics*, **27**, 215. <https://doi.org/10.1063/1.1722347>
- [16] Muller, E.W. and Tsong, T.T. (1969) *Field Ion Microscopy, Principles and Applications*. Elsevier, New York.
- [17] Gomer, R. (1952) Velocity Distribution of Electrons in Field Emission Resolution in the Projection Microscope. *The Journal of Chemical Physics*, **20**, 1772.
- [18] Derochette, J.M. and Marien, J. (1977) Field Emission Study of Hydrogen Adsorption on Smooth and Perfectly Ordered Iridium Surfaces (111) and (100) Influence of Steps and Iridium Clusters on the Surface Potential of the Hydrogen Film. *Physica Status Solidi*, **39**, 281-289. <https://doi.org/10.1002/pssa.2210390133>
- [19] Pauling, L. (1960) *The Nature of Chemical Bond*. Cornell University Press, Ithaca.
- [20] Jones, J.P. and Jones, N.T. (1976) *Surface Phenomena of Metals*, Monograph No. 28. Society of Chemical Industry, London, 263.
- [21] Jones, J.P. and Jones, N.T. (1976) Field Emission Microscopy of Gold on Single-Crystal Planes of Tungsten. *Thin Solid Films*, **35**, 83-97. [https://doi.org/10.1016/0040-6090\(76\)90243-1](https://doi.org/10.1016/0040-6090(76)90243-1)
- [22] Huber, E.E. (1966) The Effect of Mercury Contamination on the Work Function of Gold. *Applied Physics Letters*, **8**, 169.
- [23] Riviere, J.C. (1966) The Work Function of Gold. *Applied Physics Letters*, **8**, 172.
- [24] Michaelson, H.B. (1977) The Work Function of the Elements and Its Periodicity. *Journal of Applied Physics*, **48**, 4729-4733. <https://doi.org/10.1063/1.323539>
- [25] Fann, W.S., Stort, R., Tom, H.W.K. and Bokor (1992) Direct Measurement of Non-equilibrium Electron-Energy Distributions in Subpicosecond Laser-Heated Gold Films. *Physical Review Letters*, **68**, 2834-2837.
- [26] Zhao, G., Kozuka, H. and Yoko, T. (1997) Effects of the Incorporation of Silver and Gold Nanoparticles on the Photoanodic Properties of Rose Bengal Sensitized TiO<sub>2</sub> Film Electrodes Prepared by Sol-Gel Method. *Solar Energy Materials and Solar Cell*, **46**, 219-231. [https://doi.org/10.1016/S0927-0248\(97\)00005-6](https://doi.org/10.1016/S0927-0248(97)00005-6)
- [27] Eder, H., Messerschmidt, W. and Winter, H.P. (2000) Electron Emission from Clean Gold Bombarded Slow Au<sup>q+</sup> (q = 1 – 3) Ions. *Journal of Applied Physics*, **87**, 8198. <https://doi.org/10.1063/1.373519>
- [28] Kim, K., Lee, S.H., Yi, W., Kim, J. and Chio, J.W. (2003) Efficient Field Emission from Highly Aligned, Graphitic Nanotubes Embedded with Gold Nanoparticles. *Advanced Materials*, **15**, 1618-1622. <https://doi.org/10.1002/adma.200305242>
- [29] Mahmoud, A.Y., Zhang, J., Ma, D., Izquierdo, R. and Troung, V.V. (2012) Optical-Enhanced Performance of Polymer Solar Cells with Low Concentration of Gold Nanorods in the Anodic Buffer Layer. *Organic Electronics*, **13**, 3102-3107. <https://doi.org/10.1016/j.orgel.2012.09.015>
- [30] Farrer, R.A., Butterfield, F.L., Chen, V.W. and Fourkas, J.T. (2005) Highly Efficient Multiphoton-Absorption-Induced Luminescence from Gold Nanoparticles. *Nano Letters*, **5**, 1139-1142. <https://doi.org/10.1021/nl050687r>
- [31] Trouwborst, M.L., Huisman, E.H., Bakker, F.L., Van der Molen, S.J. and Van Wees, B.J. (2008) Single Atom Adhesion in Optimized Gold Nanojunction. *Physical Re-*

---

*view Letters*, **100**, 1-4.

- [32] Abid, J.P., Girault, H.H. and Brevet, P.F. (2001) Selective Structure Changes of Core-Shell Gold-Silver Nanoparticles by Laser Irradiation: Homogeneisation vs. Silver Removal. *Chemical Communications*, No. 9, 829-830.  
<https://doi.org/10.1039/b100856k>
- [33] Park, M., Chin, B.D., Yu, J.W., Chun, M.S. and Han, S.H. (2008) Enhanced Photocurrent and Efficiency of Poly (3-Hexylthiophene)/Fullerene Photovoltaic Devices by the Incorporation of Gold Nanoparticles. *Journal of Industrial and Engineering Chemistry*, **14**, 382-386. <https://doi.org/10.1016/j.jiec.2008.01.014>
- [34] Frederiksen, T., Loente, N., Paulsson, M. and Brandbyge, M. (2007) From Tunneling to Contact: Inelastic Signals in an Atomic Gold Junction from First Principles. *Physical Review B*, **75**, 1-8.
- [35] Salisbury, B.E., Wallace, W.T. and Whetten, R.L. (2000) Low-Temperature Activation of Molecular Oxygen by Gold Clusters: A Stoichiometric Process Correlated to Electron Affinity. *Chemical Physics*, **262**, 131-141.  
[https://doi.org/10.1016/S0301-0104\(00\)00272-X](https://doi.org/10.1016/S0301-0104(00)00272-X)